JCTC Journal of Chemical Theory and Computation
Article
Cite This: J. Chem. Theory Comput. 2019, 15, 4924−4932
pubs.acs.org/JCTC

# Singlet−Triplet Energy Gaps of Organic Biradicals and Polyacenes with Auxiliary-Field Quantum Monte Carlo

James Shee,[*,†] Evan J. Arthur,[‡] Shiwei Zhang,[¶,§] David R. Reichman,[†] and Richard A. Friesner[†]

[†]Department of Chemistry, Columbia University, 3000 Broadway, New York, New York 10027, United States
[‡]Schrodinger Inc., 120 West 45th Street, New York, New York 10036, United States
[¶]Center for Computational Quantum Physics, Flatiron Institute, 162 Fifth Avenue, New York, New York 10010, United States
[§]Department of Physics, College of William and Mary, Williamsburg, Virginia 23187, United States

Supporting Information

**ABSTRACT:** The energy gap between the lowest-lying singlet and triplet states is an important quantity in chemical photocatalysis, with relevant applications ranging from triplet fusion in optical upconversion to the design of organic light-emitting devices. The *ab initio* prediction of singlet−triplet (ST) gaps is challenging due to the potentially biradical nature of the involved states, combined with the potentially large size of relevant molecules. In this work, we show that phaseless auxiliary-field quantum Monte Carlo (ph-AFQMC) can accurately predict ST gaps for chemical systems with singlet states of highly biradical nature, including a set of 13 small molecules and the *ortho*-, *meta*-, and *para*- isomers of benzyne. With respect to gas-phase experiments, ph-AFQMC using CASSCF trial wave functions achieves a mean averaged error of ~1 kcal/mol. Furthermore, we find that in the context of a spin-projection technique, ph-AFQMC using unrestricted single-determinant trial wave functions, which can be readily obtained for even very large systems, produces equivalently high accuracy. We proceed to show that this scalable methodology is capable of yielding accurate ST gaps for all linear polyacenes for which experimental measurements exist, that is, naphthalene, anthracene, tetracene, and pentacene. Our results suggest a protocol for selecting either unrestricted Hartree−Fock or Kohn−Sham orbitals for the single-determinant trial wave function, based on the extent of spin-contamination. These findings pave the way for future investigations of specific photochemical processes involving large molecules with substantial biradical character.

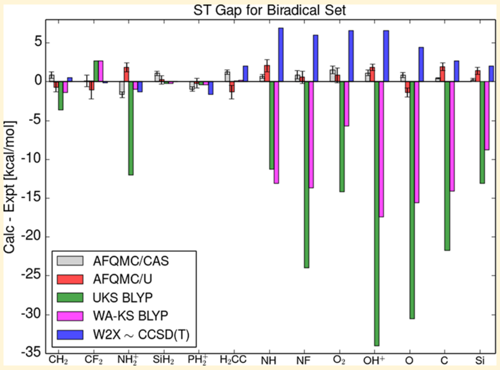

## 1. INTRODUCTION

The energy gap separating the lowest-lying singlet and triplet states of a molecule is an important property relevant to many chemical processes. For example, light absorption by chlorophyll in photosystem II can produce triplet states, which in turn react with triplet oxygen to produce short-lived and highly reactive singlet oxygen.[1] Additionally, the relative energetics of first-excited singlet and triplet states in dopants utilized in organic light-emitting diodes governs the efficiency of such devices and is a useful parameter for the design of light-emitting electronics.[2] In the field of photocatalysis the singlet−triplet (ST) gap is directly relevant to a variety of redox reactions.[3] In addition the ST gap is a quantity of crucial importance for determining the energetic feasibility of the optical processes known as singlet fission[4] and upconversion.[5] In the former process, a single photon produces a high-energy singlet state which eventually splits into two triplet excitons; in the latter, two triplet excitons annihilate or fuse to form a high energy emissive singlet. In certain cases, the ST gap can be probed under cryogenic conditions via phosphorescence measurements; however, for a large number of relevant molecules, direct measurement is not possible.

The electronic structures relevant to these types of applications can be complicated by the presence of biradical character in one or more of the involved spin states. Biradicals are molecules in which two valence electrons can occupy two degenerate but spatially distinct molecular orbitals[6] (the species are referred to as biradicaloids if these two orbitals are nearly degenerate, but we do not make this distinction here). The many possible electronic configurations give rise to their capacity to exhibit remarkably specific chemical reactivity.[7−11] Singlet states can be characterized as either closed-shell or open-shell. In the former, one of the two valence states is doubly occupied, which is typically the case, for example, in carbenes. These species can simultaneously display Lewis base and Lewis acid character and, thereby, undergo concerted addition reactions, for example, with alkenes, to produce stereospecific products. Open-shell singlet states[12] are characterized by single-occupancy of each of the two valence states, as in all triplet states due to Pauli exclusion.

**Received:** May 31, 2019
**Published:** August 5, 2019

ACS Publications

DOI: 10.1021/acs.jctc.9b00534
J. Chem. Theory Comput. 2019, 15, 4924−4932

Such open-shell molecules yield products of mixed stereochemistry.

The electronic structure community has witnessed the development of promising theoretical methods for computing the ST gap in biradical molecules. This is a challenging problem for traditional single-reference *ab initio* methods, for example, Hartree−Fock (HF) and density functional theory (DFT), as a minimal quantum-mechanical description of the wave functions corresponding to all singlet states and one triplet state ($M_s = 0$) in the two electron two orbital model is necessarily a superposition of two electronic configurations,[13,14] thus requiring more than one Slater determinant. Even for simple chemical species, such as NH and $O_2$, which have triplet ground states, the singlet spin-configuration is notoriously difficult to describe. Accurate predictions are further complicated by the requirement that static and dynamic electron correlation be well balanced, with spin-states of both multiplicities treated on equal theoretical footing. Biradical systems have been studied with DFT[15,16] and fractional spin variants,[17,18] Generalized valence bond theory,[19−22] spin-flip (SF) methods,[13,23−25] complete active space self-consistent field (CASSCF) with second-order perturbation theory,[26] multiconfiguration pair-density functional theory (pDFT),[27−31] coupled cluster (CC) methods,[32−34] doubly electron-attached equation-of-motion CC theory,[35,36] spin-extended configuration interaction (CI) with singles and doubles,[37] incremental full CI,[38] difference dedicated CI,[39−41] the particle−particle random phase approximation (pp-RPA),[14,42] the density matrix renormalization group (DMRG),[43] Yamaguchi spin projection,[44] and its recent combination with orbital-optimized MP2.[45]

In this work, we use phaseless auxiliary-field quantum Monte Carlo (ph-AFQMC)[46,47] to compute ST gaps. While imaginary-time projection is most frequently used to yield ground-state properties of a system, the formalism has also been used to accurately compute low-lying excited states of materials,[48] molecular diatomics,[49] and dipole-bound species.[50] These calculations rely on the fact that eigenfunctions of the Hamiltonian are orthogonal. In practice, when the exact eigenfunctions are unknown, ph-AFQMC calculations use a so-called "trial wavefunction" to project out orthogonal components that may be sampled along the imaginary-time random walks. For example, for the molecules with triplet ground-states relevant to this work, the energy of the lowest-lying excited singlet state can be sampled using a trial wave function with $\langle S^2 \rangle = 0$ because of its near-orthogonality to the true triplet ground-state. In the limit of an exact trial wave function, this symmetry-constraining approach would be exact.

In what follows we will show that an unrestricted single-determinant trial wave function is capable of accurately describing multireference biradical species. This is a significant result because the computational cost of CI and CASSCF calculations, despite many recent advances,[51−54] scales exponentially with system size and thus such methods are infeasible as trial wave functions for ph-AFQMC. As an example, the number of $\pi$ electrons in the polyacene series is $4n + 2$ ($n = 1, 2, \ldots$ for benzene, naphthalene, ...), which typically must be included in the active space for accurate MCSCF-based predictions. Typical CI solvers can handle up to ∼16 active electrons and orbitals, which would be insufficient for $n > 3$.

We view the ability of an electronic structure theory to accurately describe biradicals as a prerequisite for future studies of large, typically conjugated systems that catalyze photochemical processes such as upconversion. After showing that a spin-projected approach to ph-AFQMC[55] with unrestricted single-determinant trial wave functions produces accurate results for a set of strongly biradical small molecules and three benzyne isomers, we then illustrate the scalability of our approach by taking a first step toward relevant and relatively large photocatalytic molecules, namely, the polyacene series, including naphthalene, anthracene, tetracene, and pentacene. These molecules are well-studied both experimentally (with measurements available in the literature for $n = 1$−5, though not beyond) and theoretically, as they have myriad applications in organic electronics (see references in the first paragraph of ref 42). While biradical and polyradical character is predicted to be responsible for the instability of hexacene and longer acenes,[43,56] we focus on the $n = 2$−5 molecules since they are representative of the majority of molecules in our target class of photocatalysts.[3] In fact, $n = 3,4$ are known to perform upconversion,[5] and $n = 3$−5 are known singlet-fission catalysts.[4]

This work is organized as follows. Details of our computational approach are described in section 2. In section 3, we compute ST gaps for a set of 13 small organic molecules, which have singlet states of highly biradical nature, and compare them with experimental measurements. Next, we examine *ortho*, *meta*, and *para* isomers of benzyne and show that very high accuracy can be obtained with both CASSCF and single-determinant trial wave functions using a basis set of moderate size. Having shown that a single-determinant trial wave function combined with a spin projection technique is capable of accurately describing multireference biradical species, we proceed to compute ST gaps with ph-AFQMC for the increasingly large (but not necessarily biradical) systems naphthalene, anthracene, tetracene, and pentacene and compare our results with state-of-the-art electronic structure theories and experimental measurements.

## 2. COMPUTATIONAL DETAILS

The ph-AFQMC methodology is reviewed in refs 57 and 58. All calculations utilize an imaginary time step of $\Delta\tau = 0.005$ $\mathrm{Ha}^{-1}$. Walker orthonormalization, population control, and local energy measurements are carried out every 2, 20, and 20 steps, respectively. We utilize a modified Cholesky decomposition of the electron repulsion integrals (ERIs),[59] with cutoffs of $10^{-5}$ for the small molecule biradicals, and $10^{-4}$ for polyacenes, $n = 2$−4. For pentacene ($n = 5$), we use density fitting with the Weigend Coulomb-fitting basis set[60] to reduce the memory requirements of the calculation, while preserving high accuracy in energy differences.[61]

All ph-AFQMC calculations utilize single-precision floating point arithmetic, although we note that inputs, such as the trial wave function, one-electron integrals, and decomposed ERIs, are obtained using double-precision. For ionization and bond-dissociation energies of transition metal atoms and diatomics, respectively, this yielded very high accuracy while reducing the computational cost compared to double-precision calculations.[61,62] For pentacene, the largest molecule considered in this work, we verified with separate calculations in the STO-3G basis that single- and double-precision calculations gave statistically indistinguishable results.

For the small molecule biradicals, we use the aug-cc-pV*x*Z basis sets,[63] with $x$ = T, Q. Unrestricted HF (UHF), restricted HF (RHF), and its open-shell variant (ROHF), unrestricted

Kohn−Sham DFT with the B3LYP functional (UB3LYP), and CASSCF trial wave functions are obtained using PySCF.[64] ST gaps are extrapolated to the complete basis set (CBS) limit using exponential and $1/x^3$ forms for the mean-field and correlation energies, respectively, as detailed in, for example, ref 61.

For the benzyne isomers and polyacenes, we report ST gaps in the cc-pVTZ basis,[65] primarily for computational expedience, since pentacene has nearly 900 basis functions. For hydrocarbon systems, full CBS extrapolation typically alters the triple-$\zeta$ results by ∼1 kcal/mol or less. This empirical finding is consistent with previous studies of polyacenes using other wave function methods which show little basis set dependence.[32,42,66]

Our ph-AFQMC calculations utilize the spin-projection technique detailed in ref 55. The walkers are initialized with RHF for singlets and ROHF for triplets, which have $\langle S^2 \rangle$ of exactly 0 and 2, respectively. With an appropriate form of the Hubbard−Stratonovich transformation, this can ensure that the single-particle imaginary-time propagator preserves spin-symmetry despite the use of a (possibly) spin-contaminated unrestricted trial wave function.

In what follows, we propose a simple empirical protocol, "AFQMC/U", to guide the selection of an optimal unrestricted orbital set, among UHF and UB3LYP orbitals, to be used as the trial wave function in AFQMC calculations of potentially biradical systems. UHF orbitals are used by default, unless $\langle S^2 \rangle^{\mathrm{UHF}}_{\mathrm{singlet}} > 1.1$ or $\langle S^2 \rangle^{\mathrm{UHF}}_{\mathrm{triplet}} > 2.1$, in which case UB3LYP orbitals are utilized. Our rationale is based on the observation that wave functions constructed from unrestricted Kohn−Sham orbitals are known to exhibit less spin-contamination compared to UHF solutions.[67] To justify the selected thresholds, we note that for a perfect singlet biradical, as exemplified by the dissociated $H_2$ system, UHF provides a correct description of the dissociation limit, and $\langle S^2 \rangle^{\mathrm{UHF}}_{\mathrm{singlet}} = 1$.[68] This would suggest that spin-contamination in significant excess of this value may represent distortions that are irrelevant to the essential physics of singlet biradicals, and thus UB3LYP orbitals, which are less severely contaminated, are a preferable alternative. Biradical triplet states, in general, are *not* expected to exhibit spin-contamination at the UHF level, as they are typically well-described by a single determinant (the two-determinant $M_s = 0$ triplet state is not encountered due to the constraint on $\langle S_z \rangle$). Thus, any spin-contamination in significant excess of the spin-pure value of $\langle S^2 \rangle_{\mathrm{triplet}} = 2$ is likely undesirable, and in such situations, AFQMC/U utilizes a trial wave function with UB3LYP orbitals.

## 3. RESULTS AND DISCUSSION

### 3.1. Small Molecule Biradical Set.

ST gaps are computed for the set of 13 small molecules with singlet states that exhibit substantial biradical character, recently examined in ref 27. Molecular geometries for the biradical species are taken from the Supporting Information of ref 27, which used QCISD/MG3S for $CF_2$ and QCISD(T)/aug-cc-pVQZ for the rest, with unrestricted (restricted) HF references for triplet (singlet) multiplicities, respectively. ph-AFQMC results utilizing CASSCF trial wave functions are plotted in Figure 1, relative to experimental reference values, along with data provided in ref 27 for broken-symmetry DFT with the BLYP functional (UKS/BLYP), its spin-projected variant (WA-KS/BLYP), and a composite method which has been shown to produce comparable accuracy to CCSD(T)/CBS[69] (W2X). We note that we use a different reference value for $NH_2^+$, which is from a genuine experimental measurement,[70] following ref 71.

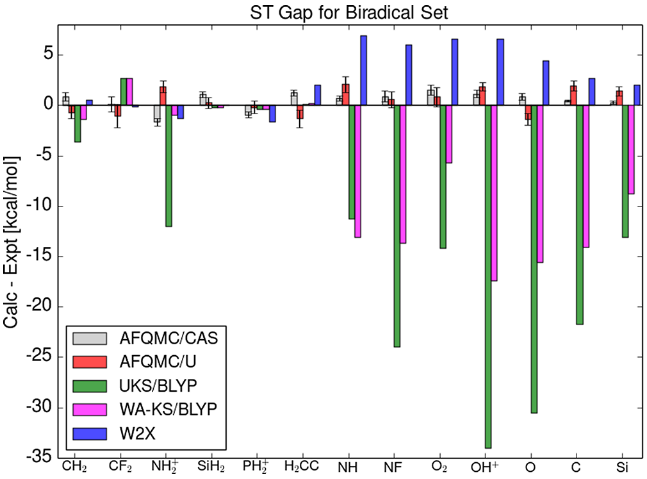

**Figure 1.** Deviations [kcal/mol] of various calculations from experimentally derived reference values. Error bars show the statistical error of the QMC measurements.

The ph-AFQMC ST gaps have been converged with respect to active space sizes of the CASSCF trial wave functions, an approach which has been shown to produce very high accuracy even for strongly correlated systems.[61,62] However, the generation of such trial wave functions is, in practice, limited to moderate system sizes due to the procedure's exponential scaling. In light of applications to large systems, such as those found in organic electronics, which we will focus on in future investigations, we explore the simplest scalable alternatives, namely, UHF and RHF wave functions, and single determinants constructed from UB3LYP orbitals. $\langle S^2 \rangle$ values with respect to the trial wave functions are shown in Table 1.

**Table 1. $\langle S^2 \rangle$ of the Singlet and Triplet Unrestricted Solutions for the 13 Small Molecule Biradical Set**

| | UHF singlet | UHF triplet | UB3LYP singlet | UB3LYP triplet |
|---|---|---|---|---|
| $CH_2$ | 0 | 2.02 | 0.57 | 2.01 |
| $CF_2$ | 0.14 | 2.01 | 0 | 2.00 |
| $NH_2^+$ | 0.82 | 2.02 | 0.75 | 2.01 |
| $SiH_2$ | 0.43 | 2.01 | 0 | 2.00 |
| $PH_2^+$ | 0.44 | 2.01 | 0 | 2.00 |
| $H_2CC$ | 0.16 | 2.35 | 0 | 2.03 |
| NH | 1.01 | 2.02 | 1.00 | 2.01 |
| NF | 1.01 | 2.02 | 1.00 | 2.01 |
| $O_2$ | 1.02 | 2.05 | 1.01 | 2.01 |
| $OH^+$ | 1.01 | 2.01 | 1.00 | 2.01 |
| O | 1.01 | 2.01 | 1.00 | 2.00 |
| C | 1.02 | 2.01 | 1.01 | 2.00 |
| Si | 1.05 | 2.02 | 1.01 | 2.00 |

Table 2 provides a rudimentary statistical representation of the accuracy of selected theoretical approaches with respect to experiment, comparing the mean signed error (MSE), mean absolute error (MAE), and maximum error (MaxE). As expected, utilizing CASSCF trial wave functions can obtain excellent accuracy, with an MAE of less than a kcal/mol and MaxE of 1.7(3) kcal/mol for $O_2$. For this molecule, we have tried active spaces of 12e8o, 8e12o, and 10e15o. The latter two active spaces produce statistically indistinguishable ST gaps in

**Table 2. Mean Signed, Absolute, and Maximum Errors [kcal/mol] of the Theoretical Methods Shown in Figure 1 for the 13 Small Molecule Biradical Set**[a]

| | MSE | MAE | MaxE |
|---|---|---|---|
| AFQMC/CAS | 0.5(4) | 0.9(4) | 1.7(3) |
| AFQMC/U | 0.5(7) | 1.2(7) | 2.1(8) |
| W2X | 2.7 | 3.1 | 6.9 |
| WA-KS/BLYP | −6.8 | 7.3 | 17.4 |
| UKS/BLYP | −12.5 | 12.9 | 34.0 |

[a] Sorted by MAE value. Parentheses indicate statistical errors.

the CBS limit. Additionally, we verified that the total energies of both the singlet and triplet states in the aug-cc-pvtz basis differ by less than 1 mHa going from one active space to the next. This suggests that the AFQMC/CAS result is converged with respect to active space size, and the remaining deviation from experiment is likely due to inaccuracies of the optimized geometries or the zero-point energies used to correct the experimental result.

The performance of UKS/BLYP is unsurprisingly poor, given the high level of spin-contamination in the singlet states revealed in Table 1. The notable onset of larger errors in Figure 1, that is, for NH, NF, $O_2$, $OH^+$, O, C, and Si, is found to roughly correlate with the presence of spin-contamination in the unrestricted wave functions. The Yamaguchi correction clearly improves upon the UKS/BLYP results; however, the MAE of 7.3 kcal/mol and MaxE of 17.4 are still very large. W2X is relatively more robust, with an MAE of 3.1 kcal/mol; however, the MaxE of 6.9 kcal/mol illustrates the difficulty in describing biradical systems even with "gold-standard" single-reference methods.

In contrast, the AFQMC/U approach shows a significant improvement in accuracy (all ph-AFQMC results using UHF, UB3LYP, and RHF trials are shown in the Supporting Information). We note that the MaxE for AFQMC/UHF is for the $H_2CC$ molecule. The UHF wave function for the triplet state, which should largely be of single-reference nature, still exhibits significant spin-contamination, as seen in Table 1. The Slater determinant derived from UB3LYP orbitals appears to be relatively uncontaminated, with an $\langle S^2 \rangle$ value of 2.03, while still benefiting from the additional variational freedom due to the use of unrestricted orbitals. When this is used as the trial wave function for ph-AFQMC, the resulting ST gap in the CBS limit is −49.9(9) kcal/mol, which significantly reduces the deviation from experiment from 3.1(7) to −1.3(9) kcal/mol. While more data points are needed to validate a more general claim, this case suggests that when a single-reference spin-state exhibits spin-contamination, AFQMC/UB3LYP can improve the accuracy of ST predictions over AFQMC/UHF. This is reflected in the protocol specified earlier for AFQMC/U, which utilizes UHF trial wave functions for triplet states when $\langle S^2 \rangle \leq 2.1$, and UB3LYP otherwise.

To make a broader comparison regarding the ability of a variety of electronic structure methods (with similar computational scaling with respect to system size) to predict ST gaps in biradicals, we include calculated values from methods highlighted in ref 14 for a subset of 8 biradicals. We plot this data in Figure 2 and provide a comparative statistical summary in Table 3.

For this subset of cases, there is no distinction between the AFQMC/UHF and AFQMC/U procedures, and AFQMC/U and AFQMC/CAS yield equivalent accuracy, considering statistical error bars. Both produce MAEs of ∼1 kcal/mol and MaxEs of ∼2 kcal/mol, comparing favorably to all other methods. As shown in the Supporting Information, the accuracy of AFQMC/UB3LYP and AFQMC/RHF is similar to that obtained via spin-flip methods for these systems.

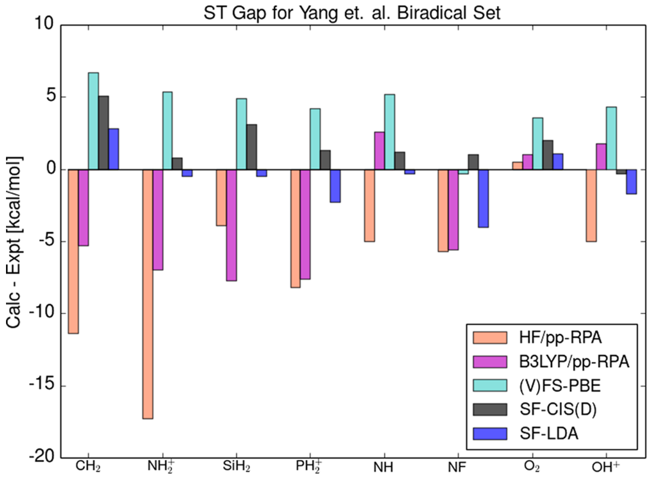

**Figure 2.** Deviations [kcal/mol] of computational methods selected from ref 14 from experimentally derived reference values, for a subset of 8 biradicals.

**Table 3. Mean Signed, Absolute, and Maximum Errors [kcal/mol] of ph-AFQMC Results and Other Methods for the 8-Molecule Biradical Subset Shown in Figure 2**[a]

| | MSE | MAE | MaxE |
|---|---|---|---|
| AFQMC/U[b] | 0.83(7) | 1.0(7) | 2.1(7) |
| AFQMC/CAS[b] | 0.5(4) | 1.1(4) | 1.7(3) |
| SF-LDA[c] | −0.7 | 1.7 | 4.0 |
| SF-CIS(D)[d] | 1.8 | 1.9 | 5.1 |
| W2X[e] | 3.0 | 3.7 | 6.9 |
| (V)FS-PBE[f] | 4.2 | 4.3 | 6.7 |
| B3LYP/pp-RPA[g] | −3.5 | 4.8 | 7.7 |
| WA-KS/BLYP[e] | −6.6 | 6.6 | 17.5 |
| HF/pp-RPA[g] | −7.0 | 7.1 | 17.3 |
| UKS/BLYP[e] | −12.5 | 12.5 | 34.0 |

[a] Sorted by MAE value. Parentheses indicate statistical errors. [b] This work. [c] SF-TDDFT with LDA functional and noncollinear kernel, TZ2P basis, from ref 72. [d] cc-pVQZ basis for NH, $OH^+$, NF, $O_2$; TZ2P basis for $CH_2$, $NH_2^+$, $SiH_2$, $PH_2^+$; from ref 13. [e] From ref 27. [f] (Variational) Fractional-Spin method, 6-311++G(2d,2p) basis, from ref 18. [g] aug-cc-pVDZ basis, from ref 14.

### 3.2. Benzyne Isomers.

In this section, we consider the *ortho-*, *meta-*, and *para-*benzyne isomers, shown in Figure 3, and compare predicted ST gaps with precise gas-phase experimental measurements. The ground state for all isomers is a singlet, and biradical character correlates with the distance between the unpaired electrons (*ortho* < *meta* < *para*).[13] These systems are of scientific interest in their own right, for example, singlet *para*-benzyne is a biradical that can abstract hydrogen atoms from specific positions in DNA, potentially enabling antitumor activity.[73,74]

*Ab initio* calculations are difficult because of the strongly correlated biradical electrons. In particular, singlet *para*-benzyne exhibits orbital instabilities at the RHF level and subsequent RHF-based correlation methods produce poor results. Better results are obtained with the broken-symmetry UHF reference, with complete spin symmetry-restoration via,

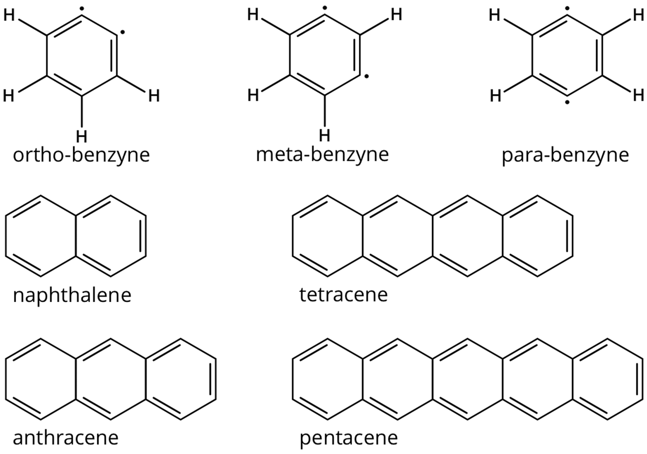

**Figure 3.** Benzyne isomers and polyacenes studied in this work.

for example, subsequent CCSD calculation.[74] With this in mind, we explore UHF and UB3LYP trial wave functions for ph-AFQMC, in addition to multideterminant trial wave functions from CASSCF.

Our ph-AFQMC calculations utilize geometries obtained from SF-DFT/6-311G* using the so-called 50/50 functional.[13] The *ortho* and *meta* geometries are provided in ref 14, and the *para* geometry is in ref 25. In ref 14, ST gaps of *para*-benzyne are based on SF-CCSD/cc-pVTZ optimized geometries.[25] However, we have performed ph-AFQMC calculations on this SF-CCSD geometry with CASSCF trial wave functions utilizing increasingly large active spaces (up to 8 electrons in 16 orbitals) and still find a residual error from experiment of 2.9(7) kcal/mol in the cc-pVTZ basis (which is altered by only 1 kcal/mol in the estimated CBS limit). For this reason and for consistency with the *ortho* and *meta* isomers, we use the SF-DFT/6-311G* geometry for the *para* isomer as well.

It is noteworthy that refs 14 and 23 do not account for ZPE contributions in comparing calculated electronic ST energies to experimentally measured quantities. For *meta*-benzyne this correction is ~1 kcal/mol, so we choose here to subtract out ZPE values, taken from ref 13, from the experimental data when comparing with purely electronic predictions.

$\langle S^2\rangle$ values of the candidate unrestricted trial wave functions are shown in Table 4 for the benzyne isomers. The UHF singlet and triplet states are both significantly contaminated in all isomers, with the singlet state of *para*-benzyne is severe case ($S^2$ = 1.68). UB3LYP reduces the amount of spin-contamination in all cases; however, it does not always eliminate it, for example, $\langle S^2\rangle$ of singlet *para*-benzyne is reduced to 0.92. The AFQMC/U method will use UB3LYP trial wave functions for all isomers, since $\langle S^2\rangle^{\text{UHF}}_{\text{singlet}} > 1.1$ for *ortho*- and *para*-benzynes, and $\langle S^2\rangle^{\text{UHF}}_{\text{triplet}} > 2.1$ for all.

**Table 4. $\langle S^2\rangle$ of the Singlet and Triplet Unrestricted Solutions for *ortho*-, *meta*-, and *para*-Benzyne Molecules**

| | UHF singlet | UHF triplet | UB3LYP singlet | UB3LYP triplet |
|---|---|---|---|---|
| *ortho* | 1.26 | 2.31 | 0.00 | 2.01 |
| *meta* | 0.97 | 2.68 | 0.10 | 2.02 |
| *para* | 1.68 | 2.31 | 0.92 | 2.01 |

The resulting ST gaps are shown in Table 5, and the deviations of the predicted values from ZPE-corrected experimental results are shown in Figure 4. AFQMC/UHF and AFQMC/UB3LYP values are shown separately in the Supporting Information.

**Table 5. ST Gaps [kcal/mol] for the *ortho*-, *meta*-, and *para*-Benzyne Isomers[a]**

| | *ortho* | *meta* | *para* |
|---|---|---|---|
| expt[b] | 37.5 ± 0.3 | 21.0 ± 0.3 | 3.8 ± 0.3 |
| ZPE[c] | −0.6 | 1.0 | 0.5 |
| ZPE-corr'd expt | 38.1 | 20.0 | 3.3 |
| AFQMC/CAS[d] | 37.4(6) | 20.7(8) | 4.5(5) |
| AFQMC/U[d] | 37.6(7) | 18.9(9) | 2.2(9) |
| UB3LYP[e] | 29.4 | 14.2 | 2.4 |
| HF/pp-RPA[f] | 45.6 | 35.5 | 4.0 |
| B3LYP/pp-RPA[f] | 37.4 | 22.1 | 0.6 |
| SF-CIS(D)[g] | 35.7 | 19.4 | 2.1 |
| SF-B3LYP[h] | 46.9 | 26.1 | 6.9 |
| SF-CCSD(T)[i] | 37.3 | 20.6 | 4.0 |
| SF-oo-CCD[g] | 37.6 | 19.3 | 3.9 |

[a] Parentheses indicate statistical errors. [b] Ref 75. [c] SF-DFT/6-311G*, ref 13. [d] SF-DFT/6-311G* geometries from ref 13, cc-pVTZ basis. This work. [e] 6-31G* basis, ref 23. [f] Ref 14. pp-RPA calculations in aug-cc-pVDZ basis. o- and m-geometries from SF-DFT with the 50/50 functional (ref 23). p-geometry from SF-CCSD, ref 25. [g] SF-DFT/6-311G* geometries, cc-pVTZ basis, ref 13. [h] cc-pVTZ basis, ref 25. [i] SF-DFT/6-311G* geometries, cc-pVTZ basis, ref 76.

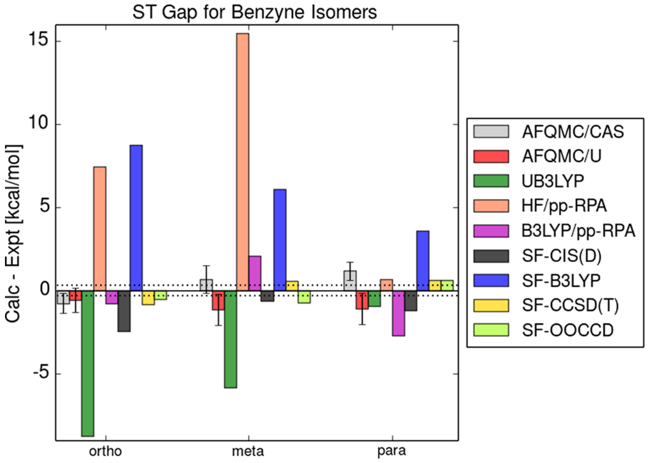

**Figure 4.** Deviations [kcal/mol] of various calculations from ZPE-corrected experimental measurements. Error bars show the statistical error of the QMC measurements. Dotted black lines represent the reported uncertainty of the experimental measurements.

SF-oo-CCD and SF-CCSD(T) both consistently obtain sub-kcal/mol accuracy, however they are computationally infeasible for larger systems due to the respective $O(M^6)$ and $O(M^7)$ scaling. We, thus, focus presently on methods with lower scaling.

AFQMC/CAS and AFQMC/U produce predictions of comparable accuracy, with maximum errors just outside 1 kcal/mol. AFQMC/UHF achieves good accuracy for the *ortho* and *meta* isomers; however, the severely spin-contaminated singlet state of *para*-benzyne results in a relatively large overestimation of the ST gap. For this latter system AFQMC/UB3LYP substantially reduces the deviation from experiment from 5.7(8) to 1(1) kcal/mol, and we note that similarly pronounced corrections are observed in pp-RPA calculations when the B3LYP reference for the $(N-2)$-electron system is used instead of HF.[14] AFQMC/U and AFQMC/UB3LYP are equivelent for this set of molecules, and thus, we again find that AFQMC/U, utilizing only unrestricted single-determinant trials, can produce results of comparable accuracy to both AFQMC/CAS and experiment.

We must emphasize the importance of explicitly breaking the spin-symmetry when obtaining UHF and UB3LYP trial wave functions, and choosing the solution with lowest-energy. For instance, the calculated ST gap using a spin-pure ($\langle S^2 \rangle = 0$) B3LYP trial for *para*-benzyne is −15 kcal/mol vs +2.2 kcal/mol when the lower-energy $\langle S^2 \rangle = 0.92$ unrestricted singlet state is used.

As a final remark in this section, we note that while indeed the errors from UB3LYP (i.e., without subsequent QMC) are generally reduced in comparison with those from the small molecule biradical set, we still find significant errors of −8.7, −5.8, and −0.9 kcal/mol for the *ortho*-, *meta*-, and *para*-benzynes. UB3LYP systematically underestimates the ST gaps because of the unrealistically low energy of the broken-symmetry singlet state. Rather unexpectedly, however, the magnitude of the errors here are inversely correlated with diradical character.

These results suggest that for the benzyne isomers, which exhibit strong biradical character, while sharing features similar to the planar aromatic ring systems relevant to chemical photocatalysis, the ST gaps are accurately predicted by ph-AFQMC with both CASSCF and single-determinant trials, and in the cc-pVTZ basis. The accuracy of AFQMC/UHF, even in its spin projected form, is compromised by the heavily spin-contaminated singlet state in *para*-benzyne, though AFQMC/UB3LYP provides an improved prediction and is utilized in our AFQMC/U method.

**Table 6. $\langle S^2 \rangle$ of the Singlet and Triplet Unrestricted Solutions for Polyacenes $n = 2-5$**

| $n$ | UHF singlet | UHF triplet | UB3LYP singlet | UB3LYP triplet |
|---|---|---|---|---|
| 2 | 1.10 | 2.30 | 0 | 2.02 |
| 3 | 1.78 | 2.68 | 0 | 2.02 |
| 4 | 2.43 | 2.91 | 0 | 2.03 |
| 5 | 3.06 | 3.44 | 0 | 2.03 |

### 3.3. Polyacenes.

Having shown that AFQMC/U can accurately describe molecules with strong biradical nature, we now show that this computational approach can scale to larger molecules, focusing on polyacenes from naphthalene to pentacene, shown in Figure 3. These molecules all have singlet ground states. We use geometries from ref 77 for the acenes, which were computed at the unrestricted B3LYP/6-31G(d) level of theory.

Table 6 shows that the extent of spin-contamination in the singlet UHF states increases with the number of fused rings. In contrast, wave functions constructed from UB3LYP orbitals are spin-pure, consistent with previous computational studies.[32,33,78]

ST gaps calculated with ph-AFQMC in the cc-pVTZ basis are shown in Table 7, alongside predictions from state-of-the-art *ab initio* methods and available experimental data. When more than one experimental value is given in ref 66, we choose the value that is closest to that shown in ref 42. Zero-point energy corrections, which are subtracted out of the experimental values, are required to compare calculated electronic energies with experiment, and we utilize numbers from ref 66 derived from B3LYP/6-31G(d) geometry optimizations and frequency calculations.

It is important to recognize that all the experimental values, except in the case of anthracene, *cannot* be fairly compared directly with gas-phase calculations. Ref 33 conveniently provides details of many of the experimental measurements, which are reproduced here. While the adiabatic ST gap of anthracene was obtained via gas-phase photoelectron spectroscopy, the reported experimental measurement for naphthalene was done in ether−isopentane−alcohol (solid) solvents at 77 K. The tetracene measurement was done in poly(methyl methacrylate) matrix at 298 K, and pentacene was measured in a tetracene matrix at 298 K. Clearly, the gas-phase 0 K conditions assumed in our calculations are not consistent with the realistic experimental conditions for most of the polyacenes studied here.

We observe that the ph-AFQMC predictions are insensitive to the trial wave function used for these polyacene systems, and show results from UHF, RHF, and UB3LYP trial wave functions in the Supporting Information. Given that naphthalene through pentacene exhibit little biradical character,[42] the extreme spin-contamination of the UHF solutions shown

**Table 7. ST Gaps [kcal/mol] for the Polyacenes $n = 2-5$[a]**

| | naphthalene | anthracene | tetracene | pentacene |
|---|---|---|---|---|
| expt[b] | [60.9] 61.0 | [42.6] 43.1 | 29.4 | 19.8 ± 0.7 |
| ZPE[b] | −3.4 | −2.3 | −1.8 | −1.5 |
| ZPE-corr'd expt | 64.4 | 45.4 | 31.2 | 21.3 |
| AFQMC/U[c] | 68.0 (1.2) | 46.2 (1.2) | 34.0 (1.6) | 25.2 (1.6) |
| UB3LYP[d] | 62.6 | 41.8 | 27.7 | 17.9 |
| CCSD(T)/FPA[e] | 65.8 | 48.2 | 33.5 | 25.3 |
| B3LYP/pp-RPA[f] | 66.2 | 45.7 | 32.1 | 22.6 |
| GAS-pDFT (FP-1)[g] | 70.6 | 45.5 | 33.6 | 25.4 |
| GAS-pDFT (WFP-3)[g] | 64.7 | 43.1 | 28.8 | 20.5 |
| ACI-DSRG-MRPT2[h] | 62.2 | 43.2 | 28.3 | 18.0 |
| DMRG-pDFT[i] | 67.1 | 46.1 | 31.6 | 22.6 |

[a] Square brackets indicate alternate experiments, and parentheses indicate statistical errors. [b] Taken from ref 66. [c] This work. [d] UB3LYP/6-31G(d) geometries and energies, ref 43. [e] B3LYP/cc-pVTZ geometries, ref 33. [f] UB3LYP/6-31G* geometries, B3LYP reference, cc-pVDZ basis, ref 42. [g] UB3LYP/6-31G(d,p) geometries, tPBE/6-31G(p,d). Active spaces defined in ref 29. [h] UB3LYP/6-31G(d) geometries, ref 66. [i] UB3LYP/6-31G(d,p) geometries. tPBE/6-31+G(p,d), ref 31.

in Table 6 is likely *not* representative of strong electron correlation, and hence restricted trial wave functions can also be expected to yield accurate results. Moreover, all ph-AFQMC variants unambiguously achieve high accuracy with respect to the gas-phase measurement for anthracene. The ph-AFQMC predictions for the other polyacenes, which were experimentally probed in (solid) solvent matrix, appear to systematically overestimate the experimental values by a few kcal/mol. For naphthalene, we performed ph-AFQMC calculations with CASSCF(10e,10o) trial wave functions, which gave a ST gap of 67(1) kcal/mol. This value is in agreement with that from AFQMC/U, given statistical error bars, and lies above the reported ZPE-corrected experiment by some 3 kcal/mol. Very similar overestimations by AFQMC/U are seen for $n = 2,4,5$ and are corroborated by CCSD(T)/FPA, B3LYP/pp-RPA, and DMRG-pDFT (though not by UB3LYP and ACI-DSRG-MRPT2). Thus, it seems reasonable to hypothesize that the calculations' neglect of molecular environment may be responsible, though admittedly there are a number of other factors that might be expected to contribute. For instance, adiabatic ST gaps are known to be sensitive to the optimized geometries, which can result in variations on the order of 1−3 kcal/mol.[66]

Overall, given the uncertainties due to the treatment of temperature, solvent, and molecular geometries in these acene calculations, ph-AFQMC with single-determinant trial wave functions gives satisfactory agreement with both experiments and other highly accurate electronic structure methods and, moreover, can scale with near-perfect parallel efficiency to systems as large as pentacene in a triple-$\zeta$ basis, which has 146 electrons and 856 basis functions.

## 4. CONCLUSIONS

With CASSCF trial wave functions, ph-AFQMC can predict ST gaps with sub kcal/mol accuracy with respect to gas-phase experimental measurements for a set of 13 small molecules with singlet states of strong biradical character. However, for large systems the generation of such a trial wave function quickly becomes impractical. The main result of this work is that near-chemical accuracy for gas-phase ST gaps can also be obtained, even for strongly correlated biradical systems, with a spin-projected ph-AFQMC technique, which initializes walkers with restricted determinants while using an unrestricted single-determinant trial wave function to implement the phaseless constraint. We establish a quantitative criteria for choosing UHF or UB3LYP orbitals based on the spin-contamination of the UHF wave function, and the resulting AFQMC/U methodology is validated on the small molecule test set, the *ortho*-, *meta*-, and *para*-benzyne isomers, and all the polyacenes for which experimental results are reported (though a true gas-phase experiment is only available for anthracene). The ph-AFQMC method is shown to provide a balanced and robust approach to accurately predicting ST gaps for molecules relevant to chemical photocatalysis.

With computational cost scaling as $O(M^4)$ or lower,[79] and with near-perfect parallel efficiency,[61,62] these calculations take only minutes of wall-time on GPU-accelerated supercomputing resources. While further investigation will be required to realistically treat solvation effects, this study paves the way for future work that will focus on a large set of both known and potential photocatalysts. Another possible extension we plan to undertake in the future is the computation of spin gaps in strongly correlated solids.

## ■ ASSOCIATED CONTENT

### Ⓢ Supporting Information

The Supporting Information is available free of charge on the ACS Publications website at DOI: 10.1021/acs.jctc.9b00534.

> ph-AFQMC results separated by trial wave function type (e.g., CASSCF, UHF, UB3LYP, RHF) and total energies for naphthalene calculations (PDF)

## ■ AUTHOR INFORMATION

### Corresponding Author

*E-mail: js4564@columbia.edu.

**ORCID**

James Shee: 0000-0001-8333-8151

Richard A. Friesner: 0000-0002-1708-9342

### Notes

The authors declare no competing financial interest.

## ■ ACKNOWLEDGMENTS

J.S. acknowledges Roel Tempelaar, Joonho Lee, Mario Motta, Hao Shi, Ian Dunn, Andrew Pun, and Zack Strater for insightful discussions. This research used resources of the Center for Functional Nanomaterials, which is a U.S. DOE Office of Science Facility, and the Scientific Data and Computing Center, a component of the Computational Science Initiative, at Brookhaven National Laboratory under Contract DE-SC0012704. An award of computer time was provided by the INCITE program. This research used resources of the Oak Ridge Leadership Computing Facility, which is a DOE Office of Science User Facility supported under Contract DE-AC05-00OR22725. The Flatiron Institute is a division of the Simons Foundation. D.R.R. acknowledges support from NSF CHE 1839464, and S.Z. acknowledges from DOE DE-SC0001303.

## ■ REFERENCES

(1) Krieger-Liszkay, A. Singlet oxygen production in photosynthesis. *J. Exp. Bot.* **2004**, *56*, 337−346.

(2) Kwak, H. S.; Giesen, D. J.; Hughes, T. F.; Goldberg, A.; Cao, Y.; Gavartin, J.; Dixon, S.; Halls, M. D. In silico evaluation of highly efficient organic light-emitting materials. *Proc. SPIE* **2016**, 994119.

(3) Romero, N. A.; Nicewicz, D. A. Organic Photoredox Catalysis. *Chem. Rev.* **2016**, *116*, 10075−10166.

(4) Smith, M. B.; Michl, J. Singlet Fission. *Chem. Rev.* **2010**, *110*, 6891−6936.

(5) Zhou, J.; Liu, Q.; Feng, W.; Sun, Y.; Li, F. Upconversion Luminescent Materials: Advances and Applications. *Chem. Rev.* **2015**, *115*, 395−465.

(6) Salem, L.; Rowland, C. The Electronic Properties of Diradicals. *Angew. Chem., Int. Ed. Engl.* **1972**, *11*, 92−111.

(7) Abe, M. Diradicals. *Chem. Rev.* **2013**, *113*, 7011−7088.

(8) Moss, R. A.; Platz, M. S.; Jones, M., Jr. *Reactive Intermediate Chemistry*; John Wiley & Sons, 2004.

(9) Bourissou, D.; Guerret, O.; Gabbaï, F. P.; Bertrand, G. Stable Carbenes. *Chem. Rev.* **2000**, *100*, 39−92.

(10) Flanigan, D. M.; Romanov-Michailidis, F.; White, N. A.; Rovis, T. Organocatalytic Reactions Enabled by N-Heterocyclic Carbenes. *Chem. Rev.* **2015**, *115*, 9307−9387.

(11) Kirmse, W. *Carbene Chemistry*; Elsevier, 2013; Vol. *1*.

(12) Gopalakrishna, T. Y.; Zeng, W.; Lu, X.; Wu, J. From open-shell singlet diradicaloids to polyradicaloids. *Chem. Commun.* **2018**, *54*, 2186−2199.

(13) Slipchenko, L. V.; Krylov, A. I. Singlet-triplet gaps in diradicals by the spin-flip ap- proach: A benchmark study. *J. Chem. Phys.* **2002**, *117*, 4694−4708.

(14) Yang, Y.; Peng, D.; Davidson, E. R.; Yang, W. Singlet−triplet energy gaps for diradicals from particle−particle random phase approximation. *J. Phys. Chem. A* **2015**, *119*, 4923−4932.

(15) Bendikov, M.; Duong, H. M.; Starkey, K.; Houk, K.; Carter, E. A.; Wudl, F. Oligoacenes: theoretical prediction of open-shell singlet diradical ground states. *J. Am. Chem. Soc.* **2004**, *126*, 7416−7417.

(16) Squires, R. R.; Cramer, C. J. Electronic Interactions in Aryne Biradicals. Ab Initio Cal- culations of the Structures, Thermochemical Properties, and Singlet- Triplet Splittings of the Didehydronaphthalenes. *J. Phys. Chem. A* **1998**, *102*, 9072−9081.

(17) Ess, D. H.; Johnson, E. R.; Hu, X.; Yang, W. Singlet- Triplet Energy Gaps for Diradicals from Fractional-Spin Density-Functional Theory. *J. Phys. Chem. A* **2011**, *115*, 76−83.

(18) Peng, D.; Hu, X.; Devarajan, D.; Ess, D. H.; Johnson, E. R.; Yang, W. Variational fractional-spin density-functional theory for diradicals. *J. Chem. Phys.* **2012**, *137*, 114112.

(19) Carter, E. A.; Goddard, W. A., III Electron correlation, basis sets, and the methylene singlet−triplet gap. *J. Chem. Phys.* **1987**, *86*, 862−865.

(20) Carter, E. A.; Goddard, W. A. New predictions for singlet-triplet gaps of substituted carbenes. *J. Phys. Chem.* **1987**, *91*, 4651−4652.

(21) Carter, E. A.; Goddard, W. A., III Correlation-consistent singlet−triplet gaps in substi- tuted carbenes. *J. Chem. Phys.* **1988**, *88*, 1752−1763.

(22) Irikura, K. K.; Goddard, W., III; Beauchamp, J. Singlet-triplet gaps in substituted carbenes CXY (X, Y= H, fluoro, chloro, bromo, iodo, silyl). *J. Am. Chem. Soc.* **1992**, *114*, 48−51.

(23) Shao, Y.; Head-Gordon, M.; Krylov, A. I. The spinflip approach within time-dependent density functional theory: Theory and applications to diradicals. *J. Chem. Phys.* **2003**, *118*, 4807−4818.

(24) Krylov, A. I. Spin-Flip Equation-of-Motion Coupled-Cluster Electronic Structure Method for a Description of Excited States, Bond Breaking, Diradicals, and Trirad- icals. *Acc. Chem. Res.* **2006**, *39*, 83−91.

(25) Bernard, Y. A.; Shao, Y.; Krylov, A. I. General formulation of spin-flip time-dependent density functional theory using non-collinear kernels: Theory, implementation, and benchmarks. *J. Chem. Phys.* **2012**, *136*, 204103.

(26) Stoneburner, S. J.; Shen, J.; Ajala, A. O.; Piecuch, P.; Truhlar, D. G.; Gagliardi, L. Systematic design of active spaces for multi-reference calculations of singlet−triplet gaps of organic diradicals, with benchmarks against doubly electron-attached coupled-cluster data. *J. Chem. Phys.* **2017**, *147*, 164120.

(27) Bao, J. L.; Sand, A.; Gagliardi, L.; Truhlar, D. G. Correlated-participating-orbitals pair-density functional method and application to multiplet energy splittings of main- group divalent radicals. *J. Chem. Theory Comput.* **2016**, *12*, 4274−4283.

(28) Wilbraham, L.; Verma, P.; Truhlar, D. G.; Gagliardi, L.; Ciofini, I. Multiconfiguration pair-density functional theory predicts spin-state ordering in iron complexes with the same accuracy as complete active space second-order perturbation theory at a signifi- cantly reduced computational cost. *J. Phys. Chem. Lett.* **2017**, *8*, 2026−2030.

(29) Ghosh, S.; Cramer, C. J.; Truhlar, D. G.; Gagliardi, L. Generalized-active-space pair- density functional theory: an efficient method to study large, strongly correlated, con- jugated systems. *Chem. Sci.* **2017**, *8*, 2741−2750.

(30) Stoneburner, S. J.; Truhlar, D. G.; Gagliardi, L. MC-PDFT can calculate singlet−triplet splittings of organic diradicals. *J. Chem. Phys.* **2018**, *148*, No. 064108.

(31) Sharma, P.; Bernales, V.; Knecht, S.; Truhlar, D. G.; Gagliardi, L. Density matrix renor- malization group pair-density functional theory (DMRG-PDFT): singlettriplet gaps in polyacenes and polyacetylenes. *Chem. Sci.* **2019**, *10*, 1716−1723.

(32) Hajgató, B.; Szieberth, D.; Geerlings, P.; De Proft, F.; Deleuze, M. S. A benchmark theoretical study of the electronic ground state and of the singlet-triplet split of benzene and linear acenes. *J. Chem. Phys.* **2009**, *131*, 224321.

(33) Hajgató, B.; Huzak, M.; Deleuze, M. S. Focal Point Analysis of the SingletTriplet Energy Gap of Octacene and Larger Acenes. *J. Phys. Chem. A* **2011**, *115*, 9282−9293.

(34) W-loch, M.; Gour, J. R.; Piecuch, P. Extension of the renormalized coupled-cluster methods exploiting left eigenstates of the similarity-transformed Hamiltonian to open- shell systems: A benchmark study. *J. Phys. Chem. A* **2007**, *111*, 11359−11382.

(35) Shen, J.; Piecuch, P. Doubly electron-attached and doubly ionized equation-of-motion coupled-cluster methods with 4-particle−2-hole and 4-hole−2-particle excitations and their active-space extensions. *J. Chem. Phys.* **2013**, *138*, 194102.

(36) Ajala, A. O.; Shen, J.; Piecuch, P. Economical doubly electron-attached equation-of- motion coupled-cluster methods with an active-space treatment of three-particle−one- hole and four-particle−two-hole excitations. *J. Phys. Chem. A* **2017**, *121*, 3469−3485.

(37) Tsuchimochi, T.; Ten-no, S. Bridging single-and multireference domains for electron correlation: spin-extended coupled electron pair approximation. *J. Chem. Theory Comput.* **2017**, *13*, 1667−1681.

(38) Zimmerman, P. M. Singlet−Triplet Gaps through Incremental Full Configuration Interaction. *J. Phys. Chem. A* **2017**, *121*, 4712−4720.

(39) Garcia, V.; Castell, O.; Reguero, M.; Caballol, R. Singlet-triplet energy gap in halogen- substituted carbenes and silylenes: a difference-dedicated configuration interaction cal- culation. *Mol. Phys.* **1996**, *87*, 1395−1404.

(40) Cabrero, J.; Ben-Amor, N.; Caballol, R. Singlet- Triplet Gap in $\alpha$-n-Dehydrotoluene and Related Biradicals: An ab Initio Configuration Interaction Study. *J. Phys. Chem. A* **1999**, *103*, 6220−6224.

(41) Calzado, C. J.; Angeli, C.; de Graaf, C.; Caballol, R. Analysis of the magnetic coupling in nitroxide organic biradicals. *Theor. Chem. Acc.* **2011**, *128*, 505−519.

(42) Yang, Y.; Davidson, E. R.; Yang, W. Nature of ground and electronic excited states of higher acenes. *Proc. Natl. Acad. Sci. U. S. A.* **2016**, *113*, E5098−E5107.

(43) Hachmann, J.; Dorando, J. J.; Avilés, M.; Chan, G. K.-L. The radical character of the acenes: A density matrix renormalization group study. *J. Chem. Phys.* **2007**, *127*, 134309.

(44) Yamaguchi, K.; Jensen, F.; Dorigo, A.; Houk, K. A spin correction procedure for unrestricted Hartree-Fock and Mller-Plesset wavefunctions for singlet diradicals and polyradicals. *Chem. Phys. Lett.* **1988**, *149*, 537−542.

(45) Lee, J.; Head-Gordon, M. Two single-reference approaches to singlet biradicaloid prob- lems: Complex, restricted orbitals and approximate spin-projection combined with regularized orbital-optimized Møller-Plesset perturbation theory. *J. Chem. Phys.* **2019**, *150*, 244106.

(46) Zhang, S.; Carlson, J.; Gubernatis, J. E. Constrained Path Quantum Monte Carlo Method for Fermion Ground States. *Phys. Rev. Lett.* **1995**, *74*, 3652.

(47) Zhang, S.; Krakauer, H. Quantum Monte Carlo Method Using Phase-Free Random Walks With Slater Determinants. *Phys. Rev. Lett.* **2003**, *90*, 136401.

(48) Ma, F.; Zhang, S.; Krakauer, H. Excited state calculations in solids by auxiliary-field quantum Monte Carlo. *New J. Phys.* **2013**, *15*, No. 093017.

(49) Purwanto, W.; Zhang, S.; Krakauer, H. Excited state calculations using phaseless auxiliary-field quantum Monte Carlo: Potential energy curves of low-lying $C_2$ singlet states. *J. Chem. Phys.* **2009**, *130*, No. 094107.

(50) Hao, H.; Shee, J.; Upadhyay, S.; Ataca, C.; Jordan, K. D.; Rubenstein, B. M. Accurate Predictions of Electron Binding Energies of Dipole-Bound Anions via Quantum Monte Carlo Methods. *J. Phys. Chem. Lett.* **2018**, *9*, 6185−6190.

(51) Zgid, D.; Nooijen, M. The density matrix renormalization group self-consistent field method: Orbital optimization with the density matrix renormalization group method in the active space. *J. Chem. Phys.* **2008**, *128*, 144116.

(52) Hohenstein, E. G.; Luehr, N.; Ufimtsev, I. S.; Martínez, T. J. An atomic orbital-based formulation of the complete active space self-

consistent field method on graphical pro- cessing units. *J. Chem. Phys.* **2015**, *142*, 224103.

(53) Smith, J. E. T.; Mussard, B.; Holmes, A. A.; Sharma, S. Cheap and Near Exact CASSCF with Large Active Spaces. *J. Chem. Theory Comput.* **2017**, *13*, 5468−5478.

(54) Vogiatzis, K. D.; Ma, D.; Olsen, J.; Gagliardi, L.; de Jong, W. A. Pushing configuration- interaction to the limit: Towards massively parallel MCSCF calculations. *J. Chem. Phys.* **2017**, *147*, 184111.

(55) Purwanto, W.; Al-Saidi, W.; Krakauer, H.; Zhang, S. Eliminating Spin Contamination in Auxiliary-Field Quantum Monte Carlo: Realistic Potential Energy Curve of $F_2$. *J. Chem. Phys.* **2008**, *128*, 114309.

(56) Solà, M. Forty years of Clar's aromatic $\pi$-sextet rule. *Front. Chem.* **2013**, *1*, 22.

(57) Motta, M.; Zhang, S. Ab initio Computations of Molecular Systems by the Auxiliary- Field Quantum Monte Carlo Method. *Wiley Interdiscip. Rev. Comput. Mol. Sci.* **2018**, *8*, No. e1364.

(58) Zhang, S. Ab Initio Electronic Structure Calculations by Auxiliary-Field Quantum Monte Carlo. *Handbook of Materials Modeling: Methods: Theory and Modeling*; 2018; pp 1−27.

(59) Purwanto, W.; Krakauer, H.; Virgus, Y.; Zhang, S. Assessing Weak Hydrogen Binding on $Ca^+$ Centers: An Accurate Many-Body Study With Large Basis Sets. *J. Chem. Phys.* **2011**, *135*, 164105.

(60) Weigend, F. Accurate Coulomb-fitting basis sets for H to Rn. *Phys. Chem. Chem. Phys.* **2006**, *8*, 1057−1065.

(61) Shee, J.; Arthur, E. J.; Zhang, S.; Reichman, D. R.; Friesner, R. A. Phaseless Auxiliary-Field Quantum Monte Carlo on Graphical Processing Units. *J. Chem. Theory Comput.* **2018**, *14*, 4109.

(62) Shee, J.; Rudshteyn, B.; Arthur, E. J.; Zhang, S.; Reichman, D. R.; Friesner, R. A. On Achieving High Accuracy in Quantum Chemical Calculations of 3d Transition Metal- containing Systems: A Comparison of Auxiliary-Field Quantum Monte Carlo with Coupled Cluster, Density Functional Theory, and Experiment for Diatomic Molecules. *J. Chem. Theory Comput.* **2019**, *15*, 2346.

(63) Kendall, R. A.; Dunning, T. H., Jr; Harrison, R. J. Electron affinities of the first-row atoms revisited. Systematic basis sets and wave functions. *J. Chem. Phys.* **1992**, *96*, 6796−6806.

(64) Sun, Q.; Berkelbach, T. C.; Blunt, N. S.; Booth, G. H.; Guo, S.; Li, Z.; Liu, J.; McClain, J. D.; Sayfutyarova, E. R.; Sharma, S.; Wouters, S.; Chan, G. K. PySCF: the PythonBased Simulations of Chemistry Framework. *WIRES Comput. Mol. Sci.* **2018**, *8*, No. e1340.

(65) Dunning, T. H., Jr Gaussian basis sets for use in correlated molecular calculations. I. The atoms boron through neon and hydrogen. *J. Chem. Phys.* **1989**, *90*, 1007−1023.

(66) Schriber, J. B.; Hannon, K. P.; Li, C.; Evangelista, F. A. A Combined Selected Con- figuration Interaction and Many-Body Treatment of Static and Dynamical Correlation in Oligoacenes. *J. Chem. Theory Comput.* **2018**, *14*, 6295−6305.

(67) Baker, J.; Scheiner, A.; Andzelm, J. Spin contamination in density functional theory. *Chem. Phys. Lett.* **1993**, *216*, 380−388.

(68) Ramos-Cordoba, E.; Salvador, P. Diradical character from the local spin analysis. *Phys. Chem. Chem. Phys.* **2014**, *16*, 9565−9571.

(69) Chan, B.; Radom, L. W2X and W3X-L: Cost-Effective Approximations to W2 and W4 with kJ $mol^{-1}$ Accuracy. *J. Chem. Theory Comput.* **2015**, *11*, 2109−2119.

(70) Gibson, S.; Greene, J.; Berkowitz, J. Photoionization of the amidogen radical. *J. Chem. Phys.* **1985**, *83*, 4319−4328.

(71) Stephens, J. C.; Yamaguchi, Y.; Sherrill, C. D.; Schaefer, H. F. $\tilde{X}^3B_1$, $\tilde{a}^1A_1$, $\tilde{b}^1B_1$, $\tilde{c}^1\sum_g^+$ Electronic States of $NH_2^+$. *J. Phys. Chem. A* **1998**, *102*, 3999−4006.

(72) Wang, F.; Ziegler, T. The performance of time-dependent density functional theory based on a noncollinear exchange-correlation potential in the calculations of excitation energies. *J. Chem. Phys.* **2005**, *122*, No. 074109.

(73) Sander, W. m-Benzyne and p-Benzyne. *Acc. Chem. Res.* **1999**, *32*, 669−676.

(74) Crawford, T. D.; Kraka, E.; Stanton, J. F.; Cremer, D. Problematic p-benzyne: Orbital instabilities, biradical character, and broken symmetry. *J. Chem. Phys.* **2001**, *114*, 10638−10650.

(75) Wenthold, P. G.; Squires, R. R.; Lineberger, W. Ultraviolet Photoelectron Spectroscopy of the o-, m-, and p-Benzyne Negative Ions. Electron Affinities and Singlet- Triplet Splittings for o-, m-, and p-Benzyne. *J. Am. Chem. Soc.* **1998**, *120*, 5279−5290.

(76) Manohar, P. U.; Krylov, A. I. A noniterative perturbative triples correction for the spin- flipping and spin-conserving equation-of-motion coupled-cluster methods with single and double substitutions. *J. Chem. Phys.* **2008**, *129*, 194105.

(77) Ibeji, C. U.; Ghosh, D. Singlet−triplet gaps in polyacenes: a delicate balance between dynamic and static correlations investigated by spin−flip methods. *Phys. Chem. Chem. Phys.* **2015**, *17*, 9849−9856.

(78) Zhang, X.; Li, Q.-S.; Xie, Y.; Schaefer, H. F., III The lowest triplet electronic states of polyacenes and perfluoropolyacenes. *Mol. Phys.* **2007**, *105*, 2743−2752.

(79) Motta, M.; Shee, J.; Zhang, S.; Chan, G. K.-L. Efficient Ab Initio Auxiliary-Field Quantum Monte Carlo Calculations in Gaussian Bases via Low-Rank Tensor Decomposition. *J. Chem. Theory Comput.* **2019**, *15*, 3510.